Identification of a Cytoplasmic Domain Important in the Polarized Expression and Clustering of the Kv2.1 K^+ Channel

Robert H. Scannevin,* Hideyuki Murakoshi,* Kenneth J. Rhodes,‡ and James S. Trimmer*

*Department of Biochemistry and Cell Biology and Institute for Cell and Developmental Biology, State University of New York, Stony Brook, New York 11794; and ‡CNS Disorders, Wyeth-Ayerst Research, Princeton, New Jersey 08543

Abstract. The voltage-sensitive K^+ channel Kv2.1 has a polarized and clustered distribution in neurons. To investigate the basis for this localization, we expressed wild-type Kv2.1 and two COOH-terminal truncation mutants, ΔC318 and ΔC187, in polarized epithelial MDCK cells. These functional channel proteins had differing subcellular localization, in that while both wild-type Kv2.1 and ΔC187 localized to the lateral membrane in high density clusters, ΔC318 was expressed uniformly on both apical and lateral membranes. A chimeric protein containing the hemagglutinin protein from influenza virus and the region of Kv2.1 that differentiates the two truncation mutants (amino acids 536–666) was also expressed in MDCK cells, where it was found in high density clusters similar to those observed for Kv2.1. Polarized expression and clustering of Kv2.1 correlates with detergent solubility, suggesting that interaction with the detergent insoluble cytoskeleton may be necessary for proper localization of this channel.

MAINTAINING spatial distribution of integral membrane proteins is a functional necessity of polarized cells. Intracellular organization of activity gives rise to directed cellular function and is essential in maintaining a multitude of tissue types. This paradigm is highly evident in neurons, where the arrangement of specialized cell surface domains is necessary to receive, integrate, and transmit both chemical and electrical information. Efficient coordination of these activities is dependent upon the precise distribution of specific ion channels to different subcellular domains (Froehner, 1993). While the fundamental molecular processes that regulate ion channel distribution have been the subject of intense investigation, the primary mechanisms responsible for differential membrane localization have been defined for only a limited number of channels (Froehner, 1993; Kim et al., 1995; Niethammer et al., 1996). Characterization of the fundamental components involved in directing and retaining channel proteins at discrete cellular locations remains a major goal of cellular and molecular neurobiology.

Voltage-sensitive potassium channels are crucial and diverse elements in the control of electrical signaling and sensitivity in excitable tissue. K^+ channels have the capacity to establish the membrane resting potential, modulate the duration and frequency of action potentials, and control neurotransmitter release (Chandy and Gutman, 1995). The high variability of K^+ channel expression, especially in the central nervous system, combined with the important aforementioned functions, has led to the proposal that differential abundance and distribution of K^+ channels confers unique excitability to different neurons (Perney and Kaczmarek, 1993). The distribution of many K^+ channel subtypes has been studied both in situ and in vivo, with spatial expression mapped to specific regions within the central nervous system. At higher resolution, the subcellular distribution of voltage-sensitive K^+ channels can be markedly distinct. Different K^+ channel subtypes (Chandy and Gutman, 1993) differentially segregate to specific neuronal membrane domains, typically being concentrated in either axons and terminals (Kv1.1 and Kv1.4; Sheng et al., 1992, 1993; Wang et al., 1993) or somatodendritic regions (Kv1.5, Kv2.1, Kv2.2, and Kv4.2; Trimmer, 1991; Sheng et al., 1992, 1994; Hwang et al., 1993; Maletic-Savatic et al., 1995; Rhodes at al., 1995), depending on cell type. Beyond the binary segregation between axonal and somatodendritic membrane domains, there appears to be present higher order sorting mechanisms. Kv2.1 is expressed only on somatic and proximal segments of dendrites in high-density clusters (Trimmer, 1991; Hwang et al., 1993; Maletic-Savatic et al., 1995; Rhodes at al., 1995), while Kv4.2 is localized to distal dendritic segments (Sheng et al., 1992). Kv1.5 and Kv2.2, however, are found homogeneously throughout the dendrite (Hwang et al., 1993; Maletic-Savatic et al., 1995). Subtype-specific sorting of highly related K^+ channels to different membrane domains indicates that highly specific cellular mechanisms exist both for generating polarized expression and for restricting lateral distribution within a given domain.

Address all correspondence to Dr. James S. Trimmer, Department of Biochemistry and Cell Biology, SUNY, Stony Brook, NY 11794-5215. Tel.: (516) 632-9171. Fax: (516) 632-8575. E-mail: trimmer@life.bio.sunysb.edu

Efforts to elucidate specific mechanisms that underlie K^+ channel distribution in neurons have been as yet unsuccessful in primary culture and in vivo. Cultured cell line models exist that in many ways can mimic the processes of neuronal cells and are more amenable to molecular manipulation (e.g., PC12 cells; see Sharma et al., 1993). Many recent studies have documented the utility of using epithelial cells to study neuronal membrane protein targeting (Rodriguez-Boulan and Powell, 1992). Although epithelia and neurons have disparate physiological functions and general morphology, they may share common molecular mechanisms for generating polarized membrane domains. Moreover, neurons are a specialized class of polarized epithelial cells. Developmentally derived from neuroepithelia, neurons ultimately acquire their specialized function through the highly localized expression of neurotransmitter receptors and ion channels. Evidence obtained from correlative targeting studies of enveloped viruses (Dotti and Simons, 1990), glypiated proteins (Dotti et al., 1991), and a neurotransmitter transporter (Pietrini et al., 1994) suggests that epithelial apical and neuronal axonal membranes, as well as epithelial basolateral and neuronal somatodendritic membranes, may be equivalent domains in regards to terminal membrane protein localization.

Here, we show that when expressed in a polarized cell line, MDCK cells, the voltage-sensitive K^+ channel Kv2.1 is localized to the lateral membrane of transfected cells, where it is found in high-density clusters. This distinctive localization in epithelia correlates with the clustered somatodendritic distribution of Kv2.1 in neurons. These data further support the hypothesis that epithelia and neurons may indeed share common molecular mechanisms for localizing and retaining membrane proteins to specific subcellular domains and allow us to use the MDCK cell line to begin to investigate the mechanisms that may be involved in the polarized, clustered expression of Kv2.1. Using this approach, we describe the characterization of a unique protein domain of the Kv2.1 polypeptide that is necessary for localization and sufficient for channel clustering in MDCK cells.

Materials and Methods

Materials

All materials not specifically identified were purchased from Sigma Chemical Co. (St. Louis, MO). Sequencing was performed with Sequenase v2.0 (United States Biochemical Corp., Cleveland, OH). Plasmid DNA used in all experiments was purified using a purification kit (Qiagen, Inc., Chatsworth, CA). All enzymes used for molecular biology were from Boehringer Mannheim Corp. (Indianapolis, IN).

Immunofluorescence of Rat Brain Sections

Adult male Sprague-Dawley rats were perfused with 4% paraformaldehyde in 0.1 M $NaPO_4$ buffer, pH 7.4 (PB), as described previously (Rhodes et al., 1995). The brains were removed, cryoprotected in 20% sucrose, frozen in dry ice, and cut into 25-μm thick sections on a sliding microtome. The sections were blocked in antibody vehicle (10 mM PB containing 0.1% Triton X-100, 4% normal goat serum), washed in PB, and then incubated overnight at 4°C in antibody vehicle containing anti-Kv2.1 antibody (KC; Trimmer, 1991) at a 1:200 dilution. The sections were then washed in 10 mM PB and incubated for 2 h at 4°C in antibody vehicle containing Texas red–conjugated goat anti–rabbit secondary antibody (Jackson ImmunoResearch Laboratories, Inc., West Grove, PA). After additional washes, the sections were mounted on silanized glass slides, air dried, and coverslipped using the ProLong antifade reagent (Molecular Probes, Eugene, OR). Immunofluorescence labeling was visualized and photographed using a photomicrography system (Axiophot; Carl Zeiss, Inc., Thornwood, NY) equipped with epifluorescence illumination.

Cell Culture and Transient Transfection

MDCK cells (kind gift of Dr. Deborah Brown, State University of New York Stony Brook, NY) were grown in DME (GIBCO-BRL, Gaithersburg, MD) supplemented with 10% FCS (Hyclone Laboratories, Logan, UT), 50 U/ml penicillin, 50 U/ml streptomycin (both GIBCO-BRL) in a humidified incubator at 37°C under 5% CO_2. Cells were maintained in either plastic tissue culture dishes or Transwell cell culture chamber inserts (No. 3412; Costar Corp., Cambridge, MA). COS-1 cells were purchased from the Microbiology Department Tissue Culture Facility (State University of New York Stony Brook, NY) and were maintained in identical media and incubation conditions using plastic tissue culture dishes.

Transient transfection of MDCK and COS-1 cells was performed by the $CaPO_4$ method (Ausubel et al., 1990). For biochemical experiments, MDCK and COS-1 cells were plated to a final confluence of 50 and 20%, respectively. For immunofluorescence experiments, MDCK and COS-1 cells were plated to a final confluence of 50 and 4%, respectively. For both types of experiments, 5–6 h after plating, cells were transfected with freshly prepared $CaPO_4$-DNA cocktail that contained the DNA of interest at a final concentration of 10 μg/ml. Proportional amounts of $CaPO_4$-DNA cocktail was added for different culture dish sizes at a ratio of 0.13 μg DNA/cm^2. 24 h after transfection, the transfection media was replaced with normal growth media. Confluent plates were processed for both protocols 24 h later. Using this procedure, a transfection efficiency of 14.2% (± 4.6%, n = 9 independent transfections) was consistently obtained. Transfection efficiency was independent of culture substrate (plastic versus Transwell membrane) and demonstrated little variability between expression constructs.

Generation of Kv2.1, ΔC318, and ΔC187 Mammalian Expression Vectors

Construction of the mammalian expression vector Kv2.1/RBG4 (= drk1/RBG4), which encodes the Kv2.1 polypeptide, is previously described (Shi et al., 1994). ΔC318/RBG4 was constructed by digesting Kv2.1/RBG4 with the restriction enzyme Tth111I. The Kv2.1 cDNA (Frech et al., 1989) is digested at two sites, once at nucleotide 1605 and again at nucleotide 3091 in the 3′ untranslated region. The 5,535-bp Tth111I fragment was gel purified from the 1,611-bp fragment and religated with T4 DNA ligase. The removal of nucleotides 1605–3091 generated a TGA stop codon after nucleotide 1605, resulting in a new construct that encoded a Kv2.1-derived polypeptide corresponding to the first 535 amino acids of Kv2.1 and lacking the COOH-terminal 318. ΔC187/RBG4 was constructed by digesting Kv2.1/RBG4 with the restriction enzymes Eco47III and BclI. These enzymes digest the Kv2.1 cDNA at nucleotides 1997 and 2973 (in the 3′UTR), respectively. The 5′ overhang from the BclI digest was filled in with the Klenow fragment to generate a blunt end. A 6,149-bp fragment was gel purified and religated (blunt to blunt). This ligation generated a TGA stop codon after nucleotide 1997. The resultant construct encodes a Kv2.1-derived polypeptide corresponding to the initial 666 amino acids of Kv2.1 and lacking the COOH-terminal 187.

Generation of Wild-Type Hemagglutinin and Hemagglutinin-2.1 Mammalian Expression Vectors

The full-length cDNA encoding for the wild-type hemagglutinin (HA)[1] polypeptide from influenza A/WSN/33 virus (kind gift from Peter Palese and Adolfo García-Sastre, Mount Sinai School of Medicine, New York) was used as a model membrane protein for transfer of function studies. A version of the HA cDNA was used that contained an introduced silent HindIII site near the COOH terminus (HA/HindIII), and was propagated in the pUC19 plasmid (Zurcher et al., 1994). A portion of the COOH terminus of HA/HindIII was subcloned in the pBluescript SK(+) phagemid (Stratagene, La Jolla, CA) HindIII to PstI to generate the pB(HACT) intermediate construct. This isolated a semiunique NsiI site at position 1725 of the HA/HindIII cDNA. The Kv2.1 cDNA was used as a template to amplify by PCR (Taq DNA Polymerase) a fragment corresponding to nu-

1. *Abbreviations used in this paper*: HA, wild-type hemagglutinin; Rh-WGA, rhodamine-conjugated wheat germ agglutinin.

cleotides 1518–1998. Additional sequence was added to the two primers 5′ of the Kv2.1 matching sequence to create NsiI restriction sites at both ends of the amplified fragment (primer 1: 5′-CCA ATG CAT ATC CCC CGA AAA GGC C-3′; primer 2: 5′-CCA ATG CAT GCT CGC AGC TTC AAG G-3′). The resultant PCR product was purified, digested with NsiI, and then ligated into pB(HACT) that had been linearized with NsiI to generate the pB(HACT-2.1) intermediate construct. Inserts in the correct orientation were verified by sequencing. The region containing the chimeric cDNA was ligated HindIII to PstI back into HA/HindIII from which the corresponding portion of the COOH terminus had been removed. The resultant chimera fused Kv2.1 amino acids 506–666 to the COOH terminus of HA. For expression in mammalian cell lines, HA-2.1 was subcloned into the RBG4 (HA-2.1/RBG4) expression vector XbaI to PstI. Additionally, full-length, HA was subcloned into RBG4 (HA/RBG4) XbaI to PstI to serve as a localization control.

Extract Preparation, Immunoprecipitation, and Immunoblotting

Immunoblotting was performed essentially as previously described (Shi et al., 1994), but with the following exceptions: Before lysis, confluent cultures were washed twice in ice-cold PBS (10 mM phosphate buffer, pH 7.4, 150 mM NaCl, containing 1 mM $MgCl_2$ and 1 mM $CaCl_2$). For detergent cell extracts, cells were lysed for 5 min on ice with ice-cold lysis buffer (150 mM NaCl, 20 mM Tris, pH 8.0, 1 mM iodoacetamide, 2 μg/ml aprotinin, 1 μg/ml leupeptin, 2 μg/ml antipain, 10 μg/ml benzamidine, and 1 mM PMSF) that contained 0.0, 0.2, 0.4, 0.6, or 1.0% Triton X-100 (vol/vol). Dishes were scraped with cell scrapers to harvest both soluble and insoluble fractions. Crude lysate was centrifuged for 10 min, 14,000 *g*, at 4°C to separate detergent soluble (lysate) and insoluble (pellet) fractions. Both fractions were resuspended in reducing SDS sample buffer to an equal volume.

For immunoprecipitation, before resuspension in sample buffer, lysate was brought to 1 ml in lysis buffer and anti-Kv2.1 antibody (pGEX-drk1; Trimmer, 1991) was added. Lysate was incubated with antibody for 3 h at 4°C while rotating, after which 25 μl of a 50% slurry of protein A–agarose (Pierce, Rockford, IL) was added and followed by rotation for 1 h at 4°C. Protein A complexes were washed six times in lysis buffer and then resuspended in reducing SDS sample buffer. Samples were heated to 80°C for 10 min, and equivalent volumes were fractionated on 9.0% polyacrylamide-SDS gels (Maizel, 1971). After electrophoretic transfer to nitrocellulose paper, blots were blocked by incubation in Blotto (4% non-fat dry milk powder in TBS [20 mM Tris, pH 7.6, 150 mM NaCl]; Johnson et al., 1984) for 1 h. This and all following incubations were performed at room temperature. Blots were immunostained with either anti-Kv2.1 antibody (pGEX-drk1) diluted 1:200 or the 2G9 mAb (kind gift from Peter Palese and Adolfo García-Sastre; Li et al., 1993) diluted 1:500 in Blotto for 1 h. Excess primary antibody was removed by washing three times for 30 min total in Blotto. Blots were then incubated for 1 h in horseradish peroxidase–conjugated goat anti–rabbit or goat anti–mouse secondary antibody (Cappel, West Chester, PA) diluted 1:2,000 in Blotto. Excess secondary antibody was removed by washing three times for 30 min in PBS. The blots were incubated in Renaissance (DuPont/New England Nuclear Boston, MA) chemiluminescence substrate and imaged on preflashed film (XOMAT LS; Eastman Kodak, Rochester, NY).

Functional Expression

24 h after transfection, MDCK cells were harvested in nonenzymatic cell dissociation solution (No. C-1544; Sigma Chemical Co.) and replated to very low density into plastic tissue culture dishes. This allows for recording from individual cells and overcomes the technical difficulty of applying the patch pipet to the apical membrane of a single cell in a monolayer. Cells were cotransfected with plasmid encoding CD8 surface antigen to identify transfected cells visually using anti-CD8 antibody–coated beads (Jurman et al., 1994). Transfection cocktails were prepared as described above with a 3:1 ratio of K^+ channel to CD8 DNA. Recordings were taken from single cells 24 h later using whole-cell patch clamp configuration (Hamill et al., 1981). Electrodes (1–3 MΩ) pulled from borosilicate glass were fire polished and filled with a solution containing 140 mM KCl, 1 mM $CaCl_2$, 10 mM EGTA, and 10 mM sodium-Hepes, pH 7.2. The bath solution contained 140 mM NaCl, 1 mM $CaCl_2$, and 10 mM sodium-Hepes, pH 7.2. Currents were recorded with a patch-clamp amplifier (EPC-7) sampled at 10 kHz on an ITC-16 A/D converter and filtered at 2 kHz by a digital bessel filter. All currents were capacity and leak subtracted using the P/6 procedure (Heinemann, 1983). All experiments were carried out at room temperature (20–24°C). The membrane potential was held at −80 mV and depolarized to +50 mV for 400 ms with 10-mV increments.

Immunofluorescence of MDCK and COS-1 Cells

MDCK cells were grown to confluence in Transwell chamber cell culture inserts. COS-1 cells were grown on poly-L-lysine–coated glass coverslips. For labeling of MDCK cells with rhodamine-conjugated wheat germ agglutinin (Rh-WGA; Molecular Probes) before fixation/permeabilization, cells were incubated for 30 min at 4°C with 20 μg/ml Rh-WGA in ice-cold PBS (10 mM phosphate buffer, pH 7.4, 150 mM NaCl, containing 1 mM $MgCl_2$ and 1 mM $CaCl_2$). Cells were then washed three times in ice-cold PBS and fixed for 30 min at 4°C in a freshly prepared 3% paraformaldehyde, 0.1% Triton X-100 solution in PBS. Excess fixative was removed by washing filters three times with PBS + 0.1% Triton X-100 (PBS-T). Nonspecific protein interactions were blocked by incubation for 30 min at room temperature in Blotto-T (4% non-fat dry milk powder in 20 mM Tris, pH 7.6, 150 mM NaCl, 0.1% Triton X-100). Cells were immunostained for 1 h at room temperature with anti-Kv2.1 antibody (pGEX-drk1) diluted 1:50 in Blotto-T or with the 2G9 mAb diluted 1:500 in Blotto-T and then washed three times in Blotto-T to remove excess primary antibody for a total of 30 min. Immunostaining was visualized by incubation with fluorescein-5-isothiocyanate–conjugated goat anti–rabbit secondary antibody (Cappel) diluted 1:2,000 in Blotto-T for 30 min at room temperature. Filamentous actin was visualized by the addition of tetramethylrhodamine isothiocyanate–conjugated phalloidin (Molecular Probes) to the secondary antibody solution to a final concentration of 125 ng/ml. Filters were washed three times in PBS-T and then mounted on slides in a 90% glycerol solution containing 0.1 mg/ml phenylenediamine in PBS, pH 9.0. Images were generated on a confocal laser scanning imaging system (model MRC-600; BioRad Labs, Hercules, CA) using a microscope (model Diaphot; Nikon, Inc., Melville, NY) with an oil immersion objective lens (60X Plan Apo; Nikon, Inc.). For all immunofluorescence images, horizontal sections through the apical and lateral domains are maximal projections of four consecutive 0.2-μm optical planes. Vertical sections are 0.2-μm line scans through the *z*-axis encompassing the entire cell (scan ~40 μm in height).

Quantitation of immunofluorescence staining was performed using NIH Image software to analyze raw confocal data. To analyze intensity distributions, average pixel intensity values were recorded from an identical square area in each of four different cell domains. Intensity values were background subtracted, and signal to noise ratios were generated by applying the following formula: $(D - E) / (I - E)$, where D is the staining intensity in the lateral or apical membrane, E is the staining intensity in the extracellular space, and I is the staining intensity within the intracellular space (nonmembrane associated). Multiple recordings were taken from multiple independent transfections for each of the constructs discussed in this manuscript. Error values were calculated by σ_{n-1} (standard deviation) analysis of each data set for each construct. A second type of intensity analysis was used to graphically illustrate the degree and magnitude of the clustering of membrane proteins. Immunostaining intensity values were measured across a 6-μm line in either the lateral or apical membrane domain, and intensity profiles were then plotted against distance. All images were magnified to the same degree, and analysis was performed on raw confocal data.

Vectorial Biotinylation of MDCK Cell Surface Proteins

Domain-specific cell surface biotinylation was performed essentially according to Gottardi et al. (1995), with the following exceptions: MDCK cells were plated to 60% confluence on Transwell filter supports and transfected 5–6 h later as described. Cells were grown for 4–5 d after transfection to establish a confluent monolayer, with media replaced every 48 h. Cells were washed three times in ice-cold PBS and then biotinylated from either the apical or basolateral side of the Transwell with biotinylation buffer (freshly dissolved Sulfo-NHS-LC Biotin [Pierce] to 1.5 mg/ml in 10 mM triethanolamine, pH 9.0, 2 mM $CaCl_2$, 150 mM NaCl). Biotinylation was performed twice, with two sequential 25-min incubations with fresh biotinylation reagent at 4°C with gentle rocking. Cells were then rinsed with PBS supplemented with 100 mM glycine for 20 min at 4°C to quench unreacted biotin. Unconjugated biotin was removed by washing three times with PBS. Cells were lysed as described above, and lysates from three duplicate Transwells were combined and then divided into two equal fractions. One half was subjected to immunoprecipitation with the

anti-Kv2.1 antibody (pGEX-drk1) as described. The remaining half of the lysate was incubated with 100 μl of a 50% slurry of streptavidin-conjugated agarose (Pierce) for 3 h at 4°C. Streptavidin agarose complexes were washed six times with lysis buffer and resuspended in reducing SDS sample buffer. Samples were heated to 80°C for 10 min, and equivalent volumes were fractionated on 9.0% polyacrylamide-SDS gels. One third of each precipitate (i.e., one half of a Transwell) was fractionated per lane. All samples were subjected to immunoblotting with anti-Kv2.1 antibody as described.

Results

Polarized Localization and Clustering of Kv2.1 in Mammalian Central Neurons

Immunofluorescence and immunohistochemical staining of sections of rat brain (Trimmer, 1991; Hwang et al., 1993; Rhodes at al., 1995) and cultured rat hippocampal neurons (Maletic-Savatic et al., 1995) demonstrate a highly ordered pattern of expression of the Kv2.1 K^+ channel polypeptide. Staining is exclusively localized to the cell soma and dendrites, with no detectable staining to axons and terminals. On dendrites, Kv2.1 immunoreactivity is limited to the proximal dendritic segments. Staining on the soma and dendrites is further confined to high-density clusters, with no observable Kv2.1 immunostaining outside of these patches. A striking example of this is the distribution of Kv2.1 in cortical pyramidal cells in rat brain sections (Fig. 1). The spatial distribution of Kv2.1 is unique among all K^+ channel subtypes examined to date and indicates that unique and precise mechanisms exist for determining the subcellular distribution of Kv2.1 in mammalian neurons.

Kv2.1, ΔC318, and ΔC187, HA, and HA-2.1 Have a Uniform Distribution in COS-1 Cells

The Kv2.1 polypeptide is distinguished among K^+ channels by its unusually long (441–amino acid) cytoplasmic tail. This region, especially the COOH-terminal 300 amino acids, is unique to Kv2.1; thus, our studies have focused on the role of this domain in mediating the subtype-specific localization of the Kv2.1 polypeptide. Two Kv2.1 truncation constructs were generated lacking portions of the cytoplasmic tail. Truncation mutant ΔC318 encodes Kv2.1 amino acids 1–535 and is thus lacking the COOH-terminal 318 amino acids. Truncation mutant ΔC187 encodes Kv2.1 amino acids 1–666 and thus lacks the COOH-terminal 187 amino acids. Additional expression constructs were generated encoding the HA protein from the influenza A/WSN/

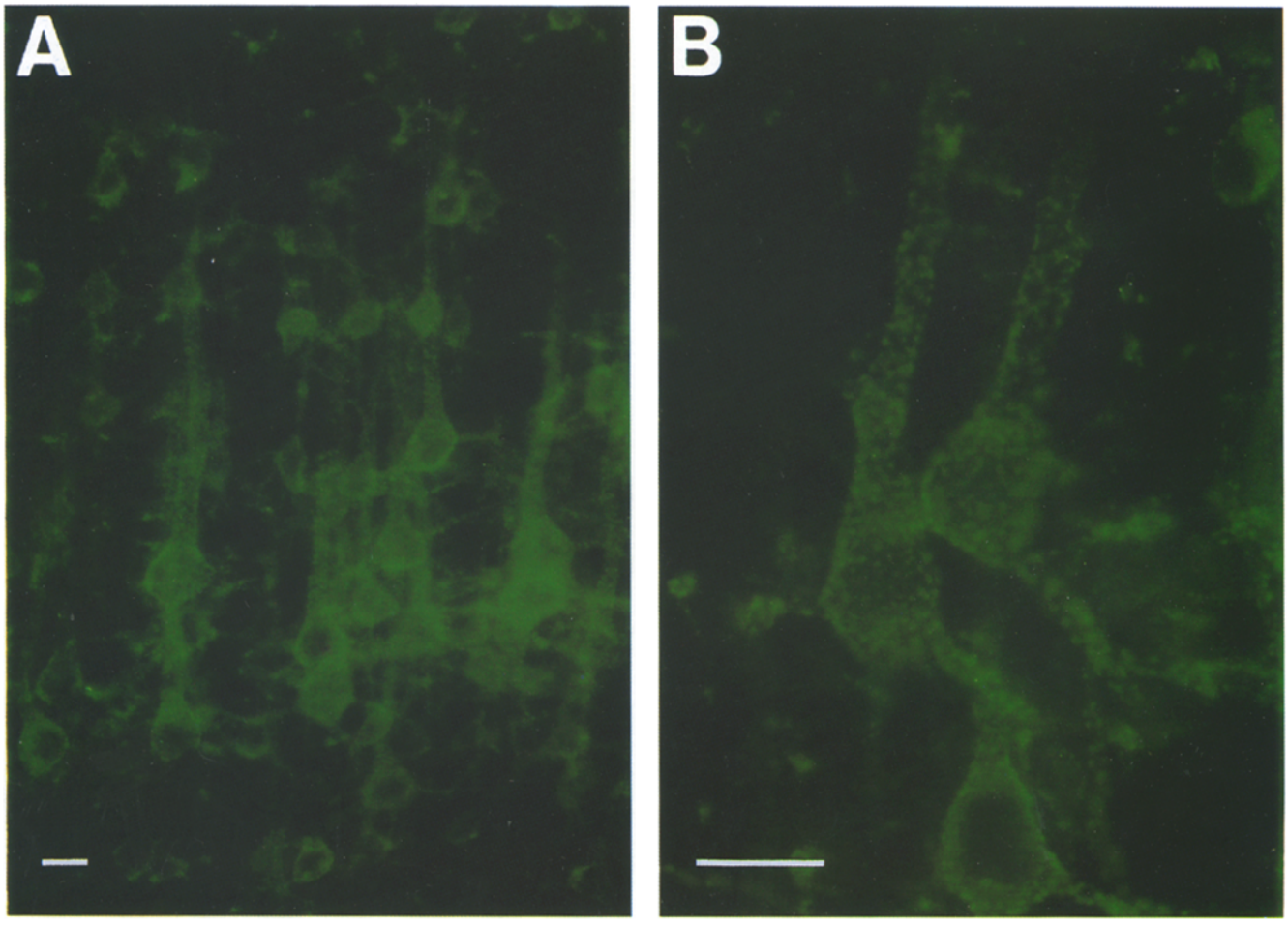

Figure 1. Immunolocalization of Kv2.1 in mammalian central neurons. Photomicrographs demonstrating (*A*) the localized expression of Kv2.1 on the cell body and proximal dendrites and (*B*) the large clusters of Kv2.1 immunoreactivity in rat neocortical pyramidal cells. The figure depicts a 25-μm section stained for immunofluorescence with anti-Kv2.1 antibody. Bars, 20 μm.

33 virus and a chimera (HA-2.1) containing the full-length HA polypeptide fused to a segment of Kv2.1 (amino acids 506–666) that contains the region that differentiates the ΔC318 and ΔC187 truncation mutants.

To determine the expression characteristics of Kv2.1, ΔC318, ΔC187, HA, and the HA-2.1 chimera, the respective expression plasmids were first transiently transfected into COS-1 cells and processed for both biochemical and immunofluorescence examination. Cell lysates from transfected cells were size fractionated by SDS-PAGE and transferred to nitrocellulose membranes for immunoblots. COS-1 cells transfected with the RBG4 vector alone expressed no anti-Kv2.1 immunoreactive bands (Fig. 2 *a*). Transfection of wild-type Kv2.1 resulted in the expression of an immunoreactive protein of 108 kD. This size is identical to the previously reported size of Kv2.1 in COS-1 cells (Shi et al., 1994). Expression of ΔC318 resulted in a major immunoreactive band of 58 kD, while expression of

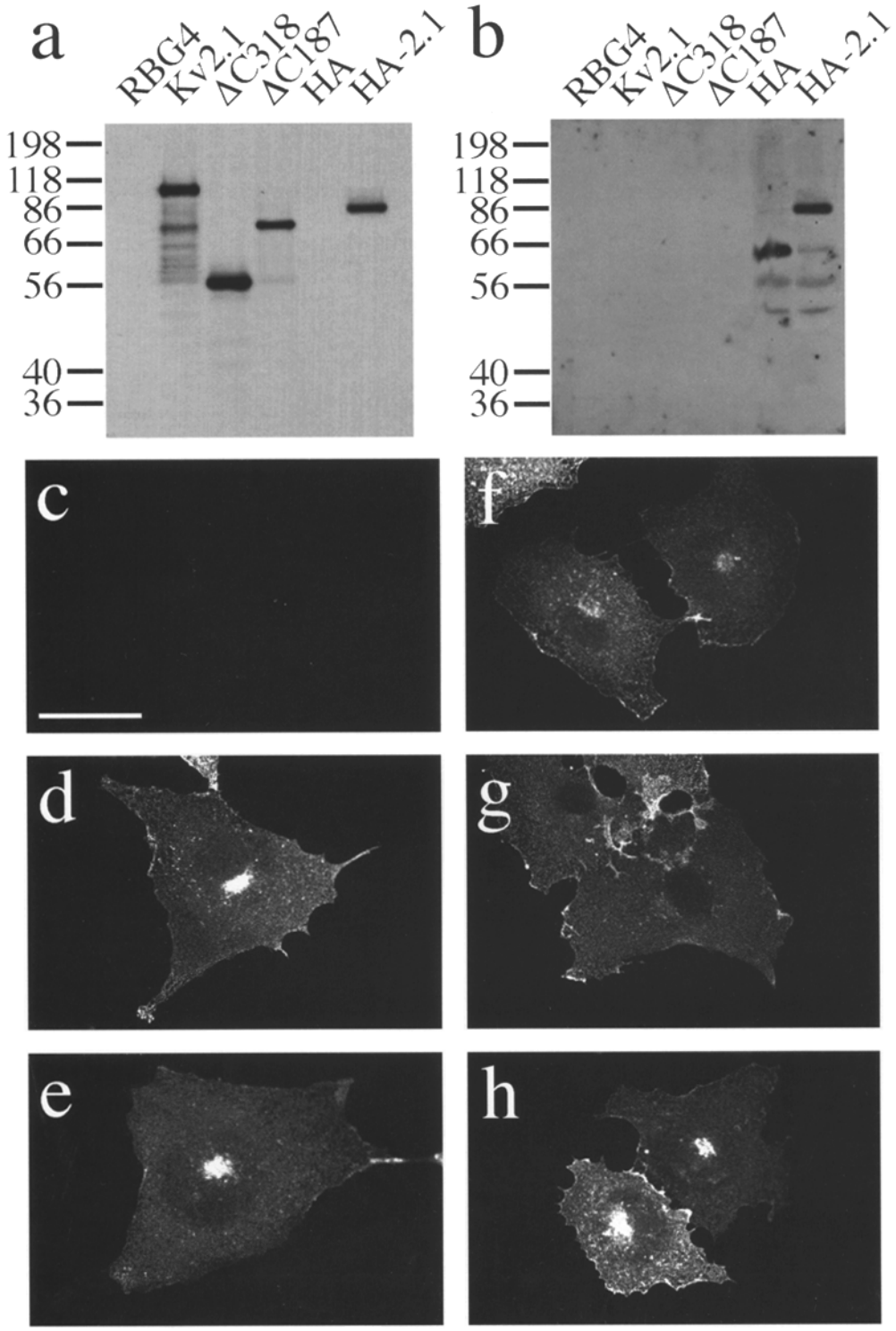

Figure 2. Kv2.1, ΔC318, ΔC187, HA, and HA-2.1 expression and immunolocalization in COS-1 cells. (*a*) Immunoblot of COS-1 lysates from cells transfected with the indicated cDNA probed with anti-Kv2.1 antibody. Numbers to left denote mobility of prestained molecular mass standards in kD. (*b*) Identical immunoblot as shown in *a*, but probed with anti-HA antibody. (*c–h*) Immunofluorescence confocal images of COS-1 cells transfected with RBG4 alone (*c*), Kv2.1 (*d*), ΔC318 (*e*), ΔC187 (*f*), HA (*g*), and HA-2.1 (*h*). Cells immunostained with anti-Kv2.1 antibody (*a–f*, *h*) or anti-HA antibody (*g*). Bar, 40 μm.

ΔC187 resulted in an immunoreactive band of ~78 kD. The HA protein was not recognized by the anti-Kv2.1 antibody, but probing a duplicate immunoblot with anti-HA antibody revealed an immunoreactive band migrating at 65 kD (Fig. 2 *b*). The chimeric protein HA-2.1 was expressed as an 85-kD band recognized by both anti-Kv2.1 and anti-HA antibodies.

Indirect immunofluorescence followed by laser scanning confocal analysis of transfected COS-1 cells revealed that transfection of RBG4 vector alone did not result in any anti-Kv2.1 or anti-HA immunofluorescence staining above typical background levels (Fig. 2 *c*, anti-HA not shown). For all other expressed cDNAs however, a similar staining pattern was observed. Transfection of Kv2.1 (Fig. 2 *d*), ΔC318 (Fig. 2 *e*), ΔC187 (Fig. 2 *f*), HA (Fig. 2 *g*), or HA-2.1 (Fig. 2 *h*) resulted in a homogenous "cell surface" staining pattern, with additional staining in the perinuclear region in what is most likely the endoplasmic reticulum. The expression pattern of these polypeptides is identical to that previously reported for Kv2.1 in COS-1 cells (Shi et al., 1994) and is typical of plasma membrane proteins expressed in COS-1 cells (Doyle et al., 1986).

Expression of Wild-Type Kv2.1, Truncation Mutants, and Chimeras in MDCK Cells

To analyze the expression of these same polypeptides in polarized epithelial cells, MDCK cells were transfected with either the RBG4 plasmid alone, or the Kv2.1, ΔC318, ΔC187, HA, or HA-2.1 expression plasmids. At 48 h after transfection, cells were harvested and subjected to immunoprecipitation with either anti-Kv2.1 or anti-HA antibodies. Proteins from equivalent samples were size fractionated by SDS-PAGE and transferred to nitrocellulose membranes for immunoblot analysis using anti-Kv2.1 antibody or anti-HA antibody. Kv2.1 isolated from native rat brain membranes (Trimmer, 1991) was also fractionated on the gel as a control for Kv2.1 immunoreactivity. MDCK cells transfected with RBG4 alone exhibited no anti-Kv2.1 immunoreactive bands (Fig. 3 *a*). This indicates that the transfection procedure itself does not induce expression of a Kv2.1-like protein, nor do MDCK cells express any endogenous proteins that cross-react with the anti-Kv2.1 antibody. MDCK cells transfected with Kv2.1 express a major immunoreactive protein of ~122 kD, which migrates

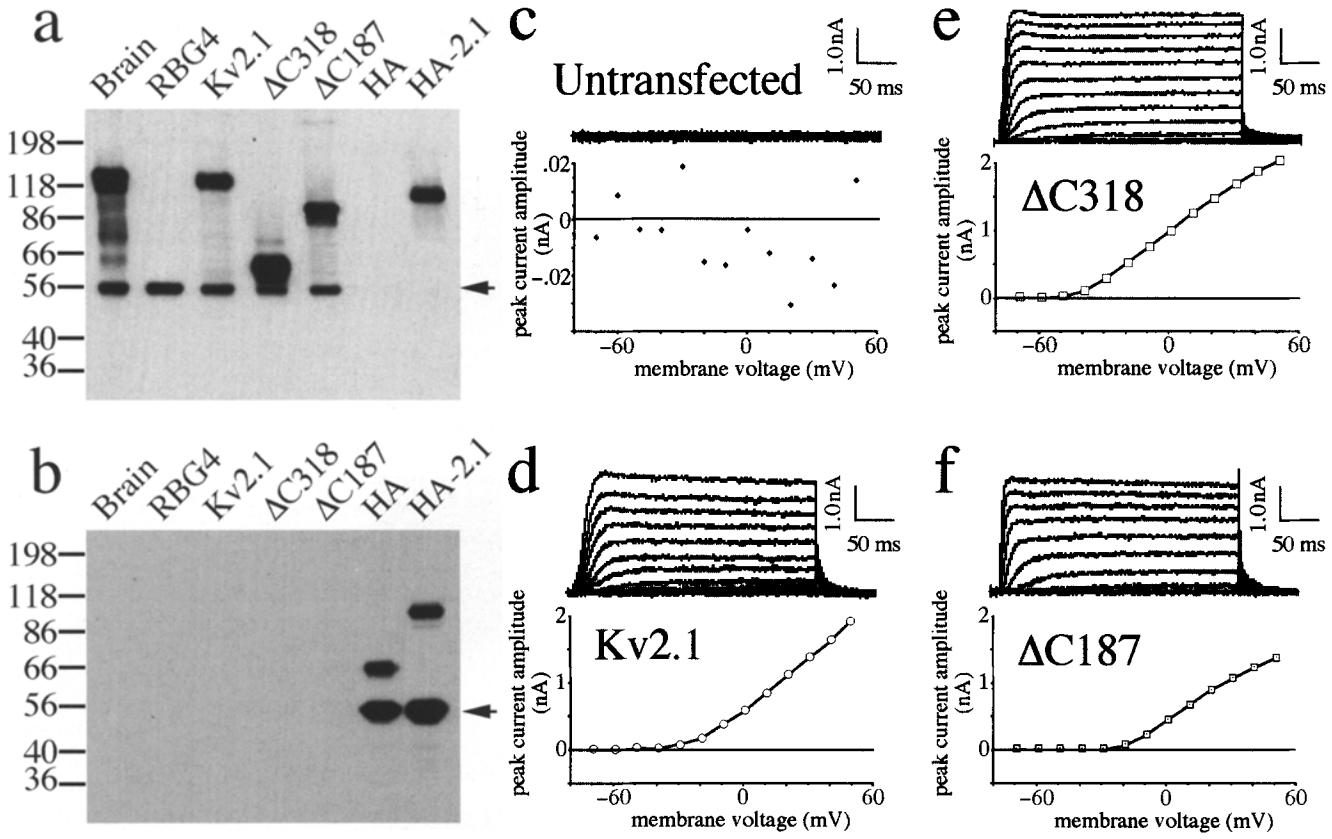

Figure 3. Kv2.1, ΔC318, ΔC187, HA, and HA-2.1 Expression in MDCK cells. (*a*) MDCK cells were transfected with the indicated cDNA. Lysates were immunoprecipitated with rabbit anti-Kv2.1 or mouse anti-HA antibody. Immunoblot was probed with anti-Kv2.1 antibody. The arrow denotes mobility of rabbit IgG heavy chain and the numbers to the left denote mobility of prestained molecular mass standards in kD. (*b*) Identical immunoblot as in *a*, but probed with mouse anti-HA antibody. The arrow denotes mobility of mouse IgG heavy chain. (*c–f*) Transfected MDCK whole cell current traces and peak current/voltage relationships evoked by +10 mV incremental voltage steps from a holding potential of −80 to +50 mV. Depolarizing pulses held for 400 ms. (*c*) Recording from untransfected MDCK cell exhibiting no voltage-sensitive currents (note different scale of I/V graph). (*d*) Recording from Kv2.1-transfected MDCK cell demonstrating noninactivating voltage-sensitive current. Threshold of activation = −30 mV. (*e*) Whole cell families of currents from ΔC318-transfected MDCK cells exhibiting noninactivating voltage-sensitive currents. Threshold of activation = −40 mV. (*f*) Noninactivating whole cell currents from ΔC187-transfected MDCK cells. Threshold of activation = −20 mV.

slightly faster than the major immunoreactive band in rat brain (132 kD; Trimmer, 1991), both of which are larger than Kv2.1 expressed in COS-1 cells (108 kD; Shi et al., 1994) and the predicted size of the core polypeptide (95 kD; Frech et al., 1989). MDCK cells transfected with ΔC318 express an immunoreactive protein of ~60 kD, which corresponds well with the predicted molecular mass of 61.6 kD, and is also similar to the size of ΔC318 from COS-1 cells. MDCK cells transfected with ΔC187 express an immunoreactive doublet, the largest of is ~90 kD, which is larger than the COS-1 form (78 kD) and the predicted molecular mass of 76.9 kD. HA-2.1 is also expressed in transfected MDCK cells and exhibited an immunoreactive band of ~105 kD, which is also larger than HA-2.1 expressed in COS-1 cells (85 kD). As in COS-1 cells, HA transfection did not result in the expression of any anti-Kv2.1 cross-reacting proteins, but probing a duplicate immunoblot with anti-HA revealed an immunoreactive band of 65 kD (Fig. 3 *b*). HA-2.1 was also evident on this blot.

For electrophysiological analysis of K^+ channel function, MDCK cells were cotransfected with the K^+ channel of interest and plasmid encoding CD8 surface antigen. Coexpression of CD8 allowed for the visual identification of transfected cells via the binding of anti-CD8 antibody–coated beads to the cell surface (Jurman et al., 1994). Instances of cotransfection were typically observed in >90% of CD8 positive cells and did not appear to have any effect on K^+ channel gating or conductance (Scannevin, R.H., and H. Murakoshi, unpublished observations). While current amplitude and threshold of activation showed variability from sample to sample, traces and current/voltage relationships shown were typical for indicated cDNA as compared to all recordings (n = 30). Whole cell patch clamp analysis of MDCK cells transfected with either Kv2.1, ΔC318, or ΔC187 revealed the expression of rapidly activating, noninactivating whole cell currents (Fig. 3, *d–f*). Untransfected MDCK cells did not exhibit any voltage-sensitive outward current in this voltage range (Fig. 3 *c*). The currents elicited by wild-type Kv2.1 and ΔC318 in these transiently transfected MDCK cells were similar to those reported previously in oocytes (Frech et al., 1989; VanDongen et al., 1990) and COS-1 cells (Shi et al., 1994). The ΔC187 truncation mutant yielded currents with similar characteristics. These results demonstrate that transiently transfected MDCK cells efficiently express and localize K^+ channels to the plasma membrane, where they are capable of conducting outward currents in a voltage-sensitive manner.

Differential Localization of Kv2.1 and Truncation Mutants in MDCK Cells Identifies a Domain Necessary for Polarized Expression and Clustering

Indirect immunofluorescence followed by confocal laser scanning microscopy was performed to determine the subcellular localization of Kv2.1, ΔC318, and ΔC187 in transfected confluent monolayers of MDCK cells grown on permeable filter supports. To facilitate the analysis of localization, before cell permeabilization with detergent, the apical membrane was labeled with Rh-WGA, followed by permeabilization and immunofluorescence analysis with the anti-Kv2.1 antibody and fluorescein-conjugated secondary antibody. As evidenced by a confocal section through the apical domain of Kv2.1 transfected MDCK cells, little or no Kv2.1 immunostaining was observed on the apical surface, while Rh-WGA staining was highly evident (Fig. 4 *a, Kv2.1*). A lateral confocal section through this same cell group revealed obvious Kv2.1 staining on the lateral membrane and no corresponding Rh-WGA labeling (Fig. 4 *b, Kv2.1*). A closer inspection of the lateral membrane revealed the clustered aspect of Kv2.1 staining in this domain (Fig. 4 *c, Kv2.1*). Confirmation of Kv2.1 localization was provided in the vertical section through this cell group, in which Kv2.1 immunostaining was observed only at the lateral membrane to the region of cell–cell contact, while Rh-WGA clearly decorated the apical surface (Fig. 4, *d* and *e, Kv2.1*). Superimposition of these two images combined with pseudocoloring revealed that there is no overlap between these two staining patterns (Fig. 4 *f, Kv2.1*). Any overlap would have been evidenced by a yellow color because of optical overlap of the red and green fluorescence. The obvious lack of basal staining is not unique to Kv2.1, as a number of MDCK "basolateral" proteins are actually highly enriched or solely expressed in lateral membranes (for examples see Gottardi and Caplan, 1993; Neam and Isacke, 1993; Zurzolo and Rodriguez-Boulan, 1993).

The subcellular localization of the Kv2.1 truncation mutant ΔC318 was determined in transiently transfected MDCK cells. A confocal section through the apical domain revealed ΔC318 immunostaining that exactly parallels the Rh-WGA labeling (Fig. 4 *a, ΔC318*). This localization pattern demonstrates that unlike wild-type Kv2.1, ΔC318 was mislocalized and expressed on the apical surface. A lateral confocal section through this same cell group revealed ΔC318 staining was also present at the lateral membrane (Fig. 4 *b, ΔC318*). A higher magnification view of this lateral membrane further clarified the homogenous staining pattern in this domain (Fig. 4 *c, ΔC318*), very different from the clustered staining observed for wild-type Kv2.1 (compare to Fig. 4 *c, Kv2.1*). The extension of ΔC318 expression onto the apical surface was highly evident in a vertical section through this cell group (Fig. 4 *d, ΔC318*). Here, ΔC318 staining was observed simultaneously on both the lateral and apical domains of the transfected cell, while Rh-WGA labeling remains restricted to the apical surface. That ΔC318 was in fact expressed on the apical membrane is shown by the superimposition of these two images, in which there is clear overlap (*yellow*) in the apical domain of the transfected cell (Fig. 4 *f, ΔC318*).

The subcellular localization of ΔC187 was also determined by immunostaining of ΔC187-transfected MDCK cells. Confocal sections through both the apical and basolateral domains of transfected cells revealed a staining pattern identical to that of wild-type Kv2.1. ΔC187 was found localized specifically to the lateral membrane (Fig. 4, *a* and *b, ΔC187*), where it was also present in high density clusters (Fig. 4 *c, ΔC187*). Vertical sectioning through this same cell group confirmed lateral localization to the region of cell–cell contact, which did not exhibit any overlap with the Rh-WGA labeling of the apical surface (Fig. 4, *d–f, ΔC187*). These results indicate that the 130 amino acids that differentiate the two truncation mutants (Kv2.1 amino

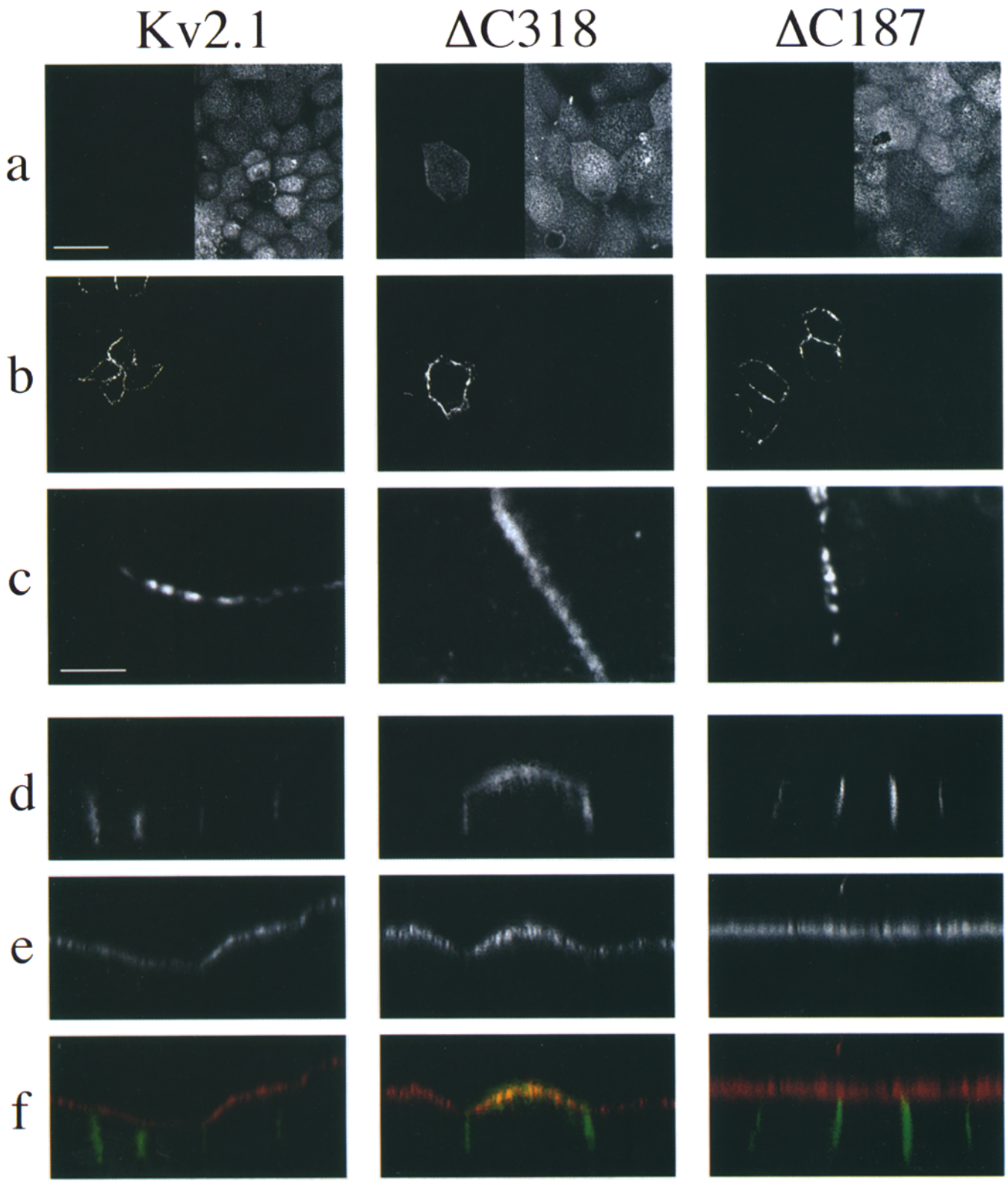

Figure 4. Immunolocalization of Kv2.1, ΔC318, and ΔC187 in MDCK cells. MDCK cells transiently transfected with Kv2.1, ΔC318, or ΔC187 were grown on Transwell filters to confluence and processed for double-label immunofluorescence confocal microscopy. Images are of the same cell group (*a–f*) for each indicated cDNA. (*a*) Horizontal confocal section through the apical domain with Kv2.1 immunostaining (*left half*) and Rh-WGA labeling (*right half*). (*b*) Horizontal confocal section through the lateral membrane with Kv2.1 immunostaining (*left half*) and Rh-WGA labeling (*right half*). (*c*) High magnification view of a lateral confocal section with Kv2.1 immunostaining. (*d*) Vertical confocal section with Kv2.1 immunostaining. (*e*) Rh-WGA labeling of identical vertical section. (*f*) Superimposition of images (*d* and *e*). Kv2.1 pseudocolored in green, Rh-WGA pseudocolored in red. Bars: (*a*) 20 μm; (*c*) 2 μm.

acids 536–666) are necessary for the restricted Kv2.1 localization to, and clustering within, the lateral membrane domain.

Experiments were also performed to determine the extent of colocalization of Kv2.1 and a number of other known lateral localizing proteins. Of particular interest was the localization pattern exhibited by filamentous actin as compared to Kv2.1. As is demonstrated in a high magnification view of the lateral membrane, Kv2.1 clusters were found interdigitated with filamentous actin clusters labeled by rhodamine-conjugated phalloidin (Fig. 5, *a–c*). This actin staining pattern did not seem to be induced by Kv2.1 expression, as untransfected cells had identical clustered staining (not shown). Kv2.1 was also found to colocalize on a gross level with fodrin and ankyrin, in that all were localized to the lateral membrane (not shown). High resolution analysis to determine the extent of colocalization with Kv2.1 (i.e., interdigitation) was inconclusive for both fodrin and ankyrin.

Domain-specific Biotinylation Confirms the Differential Localization of Kv2.1, ΔC318, and ΔC187

Steady-state cell surface biotinylation was used to confirm and quantify the localization of Kv2.1, ΔC318, and ΔC187 in MDCK cells. Confluent monolayers of transfected cells grown in Transwell filters were vectorially biotinylated from either the apical or basolateral domain. Lysates from Kv2.1-, ΔC318-, and ΔC187-transfected cells were incubated with either the anti-Kv2.1 antibody to immunoprecipitate the entire pool of channel protein, independent of biotinylation state, or with streptavidin agarose, to selectively isolate only the biotinylated protein. Equivalent samples from both isolation procedures were then analyzed on immunoblots probed with the anti-Kv2.1 antibody. Wild-type Kv2.1 was immunoprecipitated from each of the cell lysates to the same degree, regardless of biotinylation domain, while precipitation with streptavidin agarose yielded Kv2.1 only when monolayers were biotinylated from the basolateral domain (Fig. 6 *a*). This was in contrast to ΔC318, which was not only immunoprecipitated but also purified by streptavidin agarose after biotinylation of either the apical or basolateral domain (Fig. 6 *b*). ΔC318 appeared to be equally distributed between the two membrane domains, based on the relatively equal amounts of streptavidin agarose isolated protein from apical and basolateral samples. ΔC187 demonstrates the same specificity for labeling as wild-type Kv2.1, as it was only susceptible to biotinylation from the basolateral domain (Fig. 6 *c*). It is interesting to note the slight increase in M_r of Kv2.1 and ΔC187 isolated from the samples subjected to basolateral biotinylation, presumably due to the effects of covalently attached biotin on SDS gel mobility. Together, these results are in agreement with the results from the above described immunofluorescence studies in which Kv2.1 and ΔC187 have identical localizations to the basolateral membrane domain, while ΔC318 is mislocalized to the apical domain as well as the basolateral.

Immunolocalization of HA and an HA-2.1 Chimera Identifies a Domain Sufficient to Cluster Membrane Proteins

Studies were next performed to determine if the 130–amino acid region of Kv2.1 that distinguishes the properly localized ΔC187 mutant and the mislocalized ΔC318 mutant were sufficient to direct the localization and clustering of an unrelated membrane protein. Indirect immunofluorescence/confocal laser scanning microscopy was performed to determine the subcellular localization in MDCK cells of HA and HA-2.1. Immunostaining of confluent monolayers with the 2G9 mAb revealed that in transfected cells, HA protein localized specifically to the apical domain (Fig. 7 *a*) and was further characterized by a lack

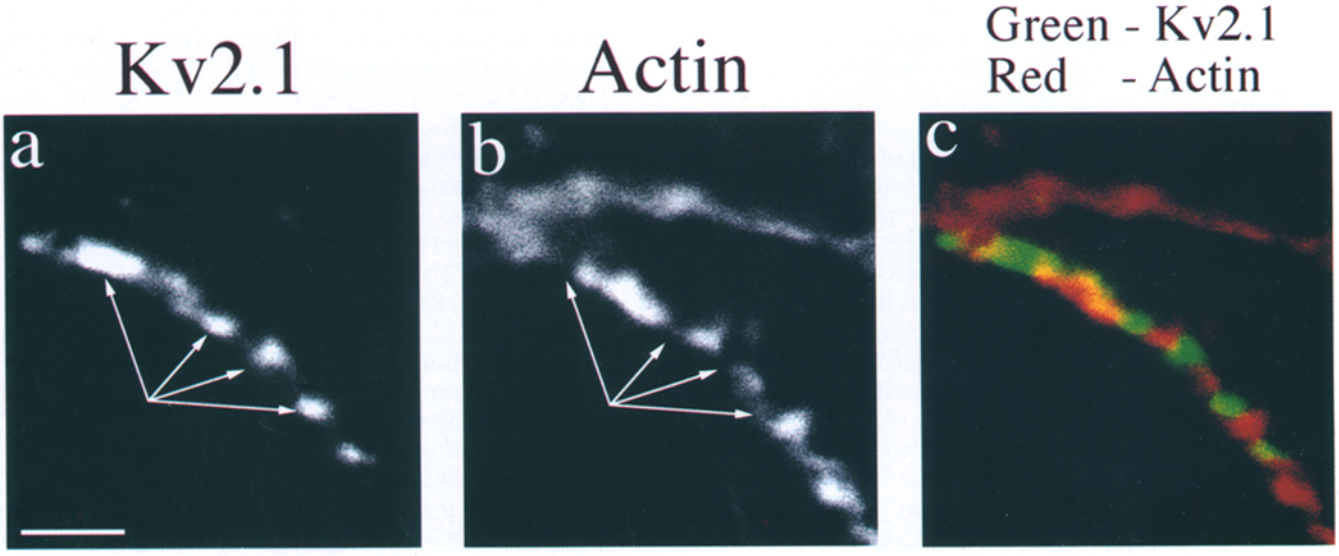

Figure 5. Localization of Kv2.1 and filamentous actin in MDCK cells. MDCK cells transiently transfected with Kv2.1 were grown to confluence on Transwell filters and processed for double-label immunofluorescence confocal microscopy. (*a*) High magnification view of a lateral membrane of a transfected cell showing Kv2.1 immunostaining. Arrows point to clusters of Kv2.1 immunostaining. (*b*) Identical cell view as in *a* of filamentous actin labeled with rhodamine-conjugated phalloidin. Arrows are in same position as in *a*, showing gaps in actin labeling. (*c*) Superimposition of images (*a* and *b*) with Kv2.1 pseudocolored in green, actin pseudocolored in red. Bar, 2 μm.

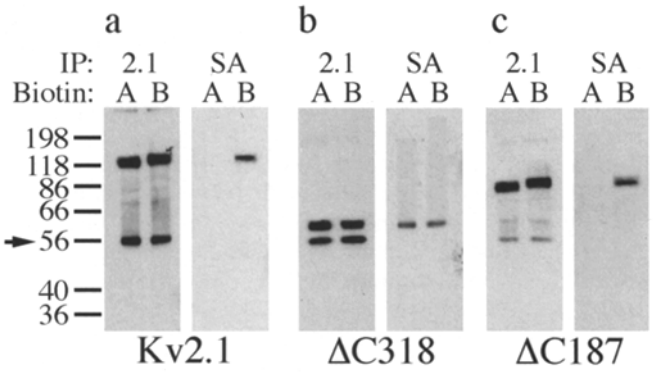

Figure 6. Vectorial biotinylation of Kv2.1, ΔC318, and ΔC187 in MDCK cells. MDCK cells were transfected with (*a*) Kv2.1, (*b*) ΔC318, or (*c*) ΔC187. Transwells of confluent transfected monolayers were biotinylated from either the apical (*A*) or basolateral, (*B*) side of the filter. Lysates from both biotinylation conditions were incubated with either anti-Kv2.1 antibody (*2.1*) or streptavidin agarose (*SA*). Immunoblot of both precipitated samples was probed with anti-Kv2.1 antibody. The arrow denotes mobility of rabbit IgG heavy chain, and numbers to the left denote migration of prestained molecular mass standards in kD.

of staining at the lateral membrane in Fig. 7 *b*. Apical localization and homogenous distribution was confirmed in a vertical confocal section through the same cell (Fig. 7 *c*). This result is consistent with localization studies performed on related HA proteins expressed in MDCK cells (Rodriguez-Boulan and Pendergast, 1980; Rodriguez-Boulan and Powell, 1992). The HA-2.1 protein, however, had a different localization in transfected cells. Immunostaining of confluent monolayers with both the 2G9 and anti-Kv2.1 antibody revealed staining at the apical surface of transfected cells localized to high-density clusters (Fig. 7 *d*), with no corresponding staining at the lateral membrane (Fig. 7 *e*). A vertical section through this same cell group confirmed the apical, clustered localization of the chimera (Fig. 7 *f*). Thus, the addition of amino acids 506–666 of Kv2.1 to the cytoplasmic COOH terminus of the HA protein is sufficient to cluster the chimeric protein at the apical domain of transfected cells, but not to redirect the chimera so that it localizes to the lateral membrane.

To extend the analysis of the degree of protein distribution between the apical and lateral membrane domains, a volume analysis on immunostaining intensity was performed. Raw confocal data from MDCK cells transfected with Kv2.1, ΔC318, ΔC187, HA, and HA-2.1 was analyzed for pixel intensity within an identical pixel area in each of four different cell domains. Relative staining intensity values were recorded from multiple transfected cells from multiple independent transfections (Table I). As is shown, the fluorescence immunostaining levels of Kv2.1 and ΔC187 in the lateral membrane were on average 40 times greater than that observed in the apical membrane. Conversely, HA and HA-2.1 revealed apical staining that was 12 and 14 times greater, respectively, than lateral staining. ΔC318 however, showed similar levels on both the apical and lateral membrane. Relatively high signal standard deviation values were observed in this analysis, presumably because of variability in protein expression, and subsequent variations in antibody binding and fluorescence. These quantitative data however, reinforce the presented immunofluorescence and biotinylation data with regards to both general polarity and specificity of localization.

To better quantify and visualize the extent of protein clustering in respective MDCK membrane domains, image analysis software was also used to quantify staining intensity. Images were magnified to the same level, and image intensity across a 6-μm line was examined. Plotting staining intensity against distance thus graphically visualized intensity profiles, and clustered proteins were easily distinguished from background fluorescence and random membrane protein surface distribution. Analysis of Kv2.1 (Fig. 8 *a*) and ΔC187 (Fig. 8 *c*) lateral membranes, as well as HA-2.1 (Fig. 8 *f*) apical membranes revealed clear peaks of intense staining that correspond to clusters. These clusters have a range of diameters ranging from 0.2 to 0.5 μm. Apical and lateral membranes from MDCK cells transfected with ΔC318 (Fig. 8, *b* and *d*) and apical membranes from cells expressing HA (Fig. 8 *e*) or labeled with Rh-WGA (Fig. 8 *g*) had a more disorganized and homogenous staining pattern, and corresponding randomly fluctuating intensity profiles. These were in contrast to the peaks of intense staining observed for Kv2.1, ΔC187, and HA-2.1; note the lack of signal in the regions between the peaks, emphasizing the efficient targeting of these polypeptides to these membrane clusters.

Detergent Insolubility of Kv2.1 in MDCK, but Not COS-1 Cells, Correlates with Polarized Expression and Clustering

As a first step toward defining cellular components present in epithelial cells that lead to the polarized expression and clustering of Kv2.1, the biochemical characterization of Kv2.1 expressed in MDCK cells were compared to Kv2.1 expressed in COS-1 cells. Previous studies have identified correlations between the detergent insolubility of membrane proteins and their subsequent proper localization in MDCK cells (Nelson and Veshnock, 1986). This is presumably due to a requirement for interaction of these proteins with detergent-insoluble components of the cytoskeleton (Morrow et al., 1989). Here, MDCK cells were transfected with Kv2.1 and subjected to extraction in various concentrations of detergent, and the detergent soluble and insoluble fractions isolated and analyzed by immunoblots. This analysis revealed that in MDCK cells, wild-type Kv2.1 was resistent to extraction, even at a relatively high concentration of Triton X-100 (1.0%; Fig. 9 *a*). The detergent solubility of Kv2.1 in COS-1 cells was markedly different, in that Kv2.1 was completely soluble even at the lowest concentration of Triton X-100 used (0.2%; Fig. 9 *a*). These results correlate with immunolocalization data, given that in MDCK cells, Kv2.1 was expressed in a polarized manner in membrane clusters, whereas in COS-1 cells expression was homogenous and uniform over the entire cell surface.

In an effort to determine the basis of Kv2.1 detergent insolubility in MDCK cells, extraction was performed on cells cultured in low Ca^{2+} media. Growth in this media leads to a loss of polarity and changes in the membrane-associated cytoskeleton such that the normally insoluble cytoskeletal complexes of ankyrin, spectrin, and E-cadherin can now be readily solubilized (Nelson and Veshnock,

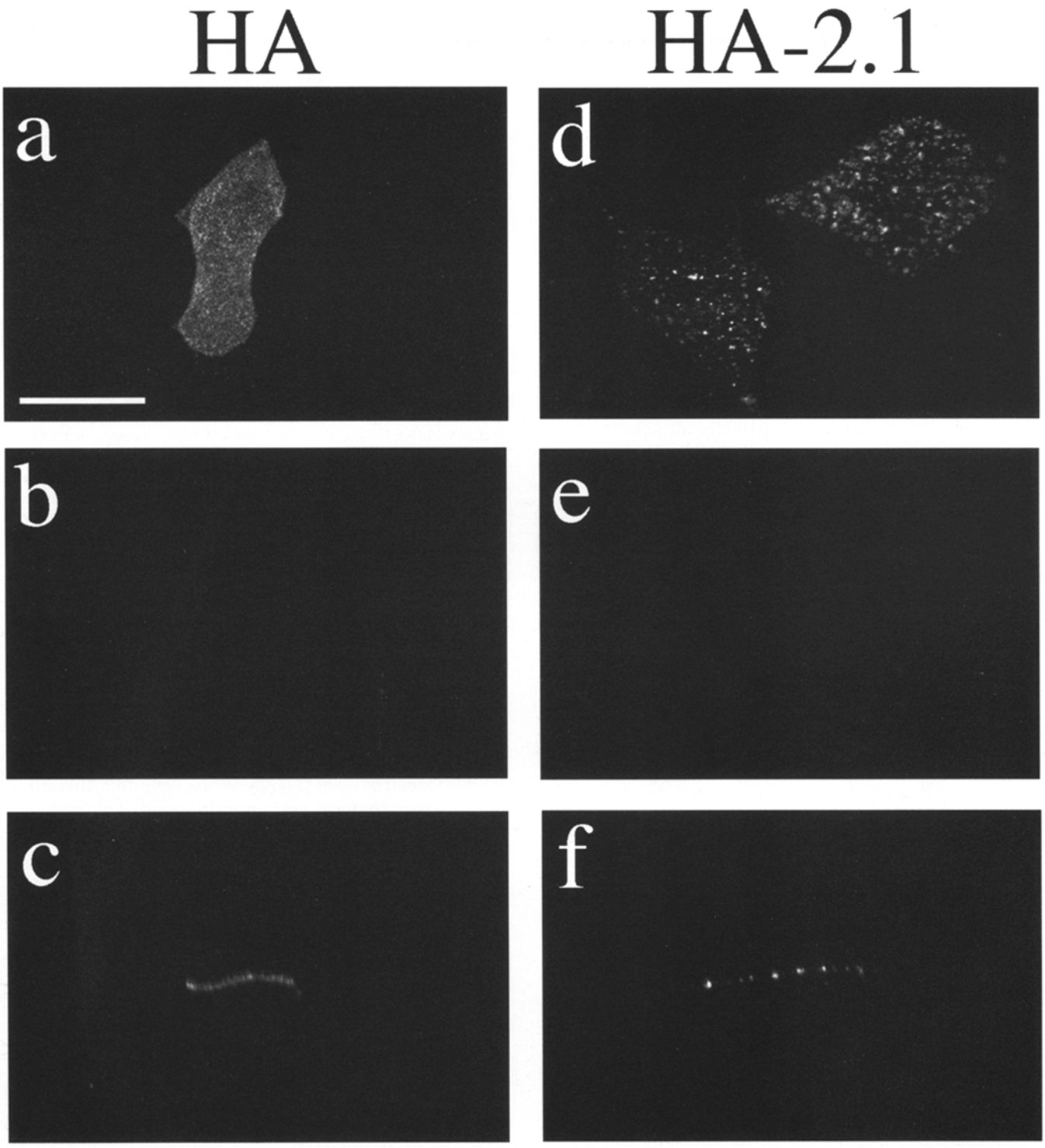

Figure 7. Immunolocalization of HA and an HA-2.1 chimera. MDCK cells were grown to confluence on Transwell filters and transiently transfected with HA (*a–c*) or HA-2.1 (*d–f*) then processed for immunofluorescence confocal microscopy. Apical confocal section through HA- (*a*), or HA-2.1- (*d*) transfected MDCK cells. (*b* and *e*) Lateral confocal section through the same cell group. (*c* and *f*) Vertical confocal section through the same cell group. Bar, 20 μm.

1987; Nelson and Hammerton, 1989; Nelson et al., 1990). MDCK cells transfected with Kv2.1 were cultured either in low or normal Ca^{2+}-containing media for 48 h. Upon detergent lysis and subsequent immunoblot analysis of equivalent fractions, the majority of Kv2.1 expressed in cells grown in low Ca^{2+} media was now in the soluble fraction, whereas from cells grown in normal media, the majority of Kv2.1 remained detergent insoluble (Fig. 9 *b*). These data suggest that Kv2.1 normally participates in a protein complex resistant to detergent extraction and that participation in this complex or association of this complex with the detergent insoluble fraction is sensitive to Ca^{2+}.

Table I. Analysis of Immunostaining Intensity in Transfected MDCK Cells

Construct	Lateral	Apical	n
Kv2.1	25.31 ± 17.66	0.66 ± 0.78	16
ΔC318	30.97 ± 25.06	26.27 ± 16.72	15
ΔC187	30.92 ± 21.36	0.73 ± 0.62	13
HA	2.06 ± 1.33	25.40 ± 11.09	14
HA-2.1	1.52 ± 1.76	21.32 ± 17.30	14

Relative signal to noise ratios for staining intensities in each of the indicated membrane domain. Ratios were calculated with the following formula: $(D - E)/(I - E)$, where D = average pixel intensity in either the lateral or apical membrane, E = average pixel intensity in the extracellular space, I = average pixel intensity in the intracellular space (nonmembrane associated). Error values shown are standard deviation calculations for each individual data set.

Discussion

The Kv2.1 delayed rectifier K^+ channel is abundantly expressed in neurons and in both skeletal and cardiac muscle. In the mammalian brain, virtually all neurons have been found to express Kv2.1. In these cells, Kv2.1 expression is highly polarized, being restricted to somatodendritic membrane domains, and is further confined to the proximal portions of the dendritic shaft (Trimmer, 1991; Hwang et al., 1993; Rhodes at al., 1995). Most if not all of the Kv2.1 staining on the plasma membrane of neurons is restricted to large, high-density clusters, which range in diameter from 0.5–1 μm (Fig. 1). While definitive ultrastructural analyses have not yet been performed, it appears that these clusters do not correspond to synapses (Rhodes, K.J., and J.S. Trimmer, unpublished observations). Kv2.1 immunostaining of cultured rat myotubes reveals the presence of similar clusters (Trimmer, J.S., unpublished observations). Patch clamp analyses of vertebrate muscle fibers have also provided evidence for nonhomogeneous expression of delayed rectifier K^+ channels. These studies showed that K^+ channels exhibit limited lateral mobility in the membrane (Almers et al., 1983) and occur in "hot spots" of activity, representing hundreds of clustered channels, with intervening regions devoid of detectable channels (Weiss et al., 1986). Kv2.1 is also expressed in a discrete pattern in the rat pheochromocytoma PC12 cell line, where it is found exclusively in high density clusters at regions of cell–cell contact, and in growth cones (Sharma et al., 1993). Together, these data point to the existence of cellular mechanisms present in many diverse cell types that can lead to the polarized, clustered expression of endogenous Kv2.1 protein.

The localization of recombinant Kv2.1 expressed in MDCK epithelial cells is in many ways similar to the expression of endogenous Kv2.1 in these diverse excitable cells. In MDCK cells, Kv2.1 is localized to the lateral membrane. Previous studies have shown that basolateral domains of polarized epithelial cells may be a functional homologue of the somatodendritic domain of neurons (Dotti

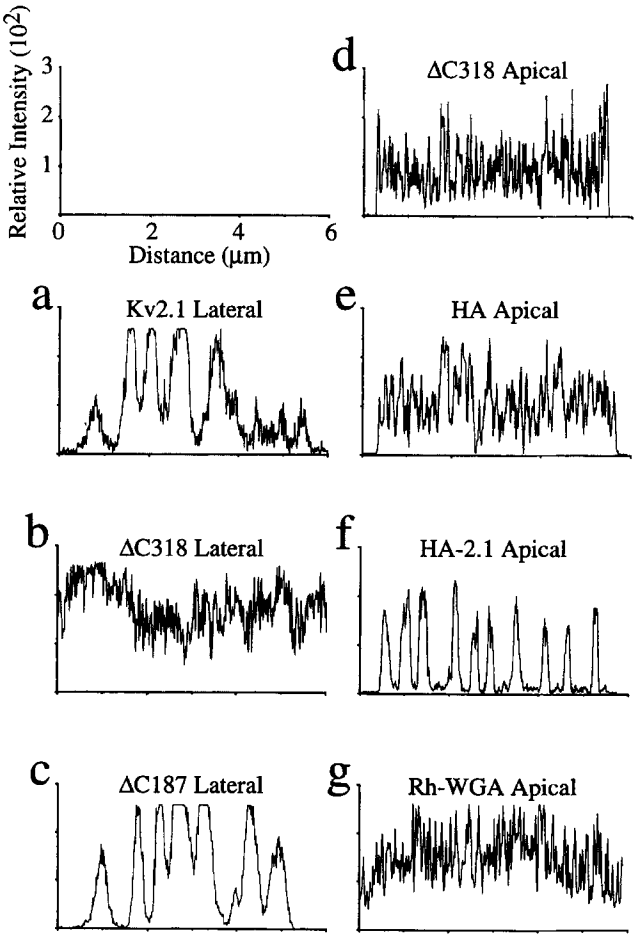

Figure 8. Clustering of proteins expressed in MDCK cells. Plots of relative staining intensity across a 6-μm line from each of the indicated transfected cell domains, Kv2.1 lateral (*a*), ΔC318 lateral (*b*), ΔC187 lateral (*c*), ΔC318 apical (*d*), HA apical (*e*), HA-2.1 apical (*f*), and Rh-WGA apical (*g*). Relative intensity values on the *y*-axis range from a low of 0 to a maximal value of 3×10^2 and are plotted against distance (in μm) on the *x*-axis.

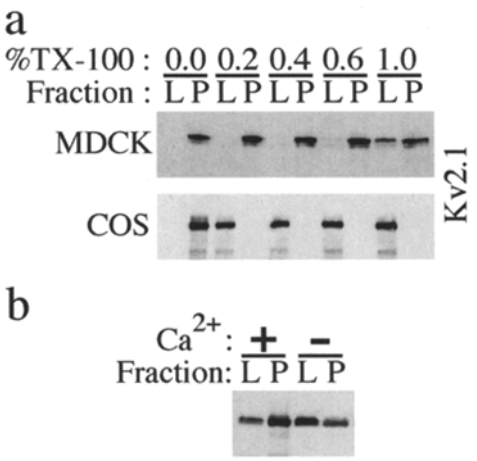

Figure 9. Detergent solubility of Kv2.1 and ΔC187 in MDCK and COS-1 cells. (*a*) MDCK and COS-1 cells were transiently transfected with Kv2.1 and then extracted in various concentrations of Triton X-100 (*%TX-100*). Equivalent volumes of detergent soluble lysate (*L*) and insoluble pellet (*P*) were analyzed by immunoblot probed with anti-Kv2.1 antibody. (*b*) Confluent monolayers of MDCK cells grown in plastic tissue culture dishes and transfected with Kv2.1 were cultured in either normal media or media containing low Ca^{2+} (Ca^{2+}: +/−). Cultures were extracted and fractionated as described in 1.0% Triton X-100 lysis buffer. Immunoblot was probed with anti-Kv2.1 antibody.

and Simons, 1990; Dotti et al., 1991; Rodriguez-Boulan and Powell, 1992; Pietrini et al., 1994). This hypothesis is further supported by the developmental origins of neurons, which arise from neuroepithelial stem cells. In this regard, the expression of Kv2.1 in the lateral membranes of MDCK cells is consistent with its polarized localization in neurons. Recombinant Kv2.1 expressed in MDCK cells is also found in clusters similar to those present in neurons, muscle fibers, and PC12 cells. Thus, it appears that both excitable and epithelial cells, but not fibroblast cells such as COS-1, contain the machinery for channel clustering, allowing for future experiments aimed at identifying the constituent components of the clustering apparatus.

Polarized localization and clustering of Kv2.1 in MDCK cells is dependent upon a 130–amino acid domain within the cytoplasmic COOH terminus of the channel protein. The necessity of this domain has been demonstrated here via deletion analysis, in that Kv2.1 mutants lacking this region are not localized specifically to the lateral membrane, nor do they form clusters. This specific localization pattern may or may not be the result of a biosynthetic sorting or targeting event. Alternative to a direct lateral targeting event concurrent with biosynthesis, it is possible that Kv2.1, ΔC187, and ΔC318 are all initially expressed in a nonpolarized fashion. Only Kv2.1 and ΔC187 are then selectively retained in clusters at the lateral membrane via interaction with one or more aspects of the endogenous MDCK lateral membrane retention machinery. ΔC318, which presumably is lacking the necessary interaction domain, does not interact and maintains a nonpolarized, nonclustered localization. That this region of Kv2.1 is sufficient for clustering is demonstrated by the localization of the HA-2.1 chimera to the apical membrane in high-density clusters. Although the chimera does not localize to the lateral membrane, it does not, however, rule out a basolateral localization signal in this domain. It may be that the basolateral signal encoded by the Kv2.1 region is masked by a stronger apical localization signal, given that the chimera contains the entire HA-coding region. Alternatively, Kv2.1-sorting signals could fail to be recognized in the chimeric protein because of biosynthetic or topological differences between the chimera and wild-type Kv2.1. It is readily apparent, however, that the Kv2.1-clustering signal is recognized and is sufficient to cluster the chimeric protein on the apical surface. To better assess the role of the Kv2.1 COOH terminus in localization in MDCK cells, it will be necessary to attach the Kv2.1 domain to a nonpolarized transmembrane protein and assay for localization. The use of a protein background for chimera construction that is lacking dominant sorting signals may help clarify the localization contribution of Kv2.1 amino acids 536–666. It should also be noted that apparently contradictory results have been obtained from some domain-deletion/chimeric protein experiments in MDCK cells (e.g., Compton et al., 1989; Brewer and Roth, 1991). One promising approach may be to construct chimeras using members of the diverse family of voltage-gated K^+ channels, which have highly conserved transmembrane and extracellular domains yet divergent cytoplasmic amino- and carboxyl termini, and divergent localization in neurons (Chandy and Gutman, 1993).

Although both Kv2.1 and ΔC187 localize to regions of cell–cell contact at the lateral membrane, contact with another cell expressing a K^+ channel on the cell surface (i.e., a homotypic interaction) does not seem to be necessary. This is evidenced by the fact that in singly transfected cells present in a field of untransfected cells, or at boundaries between multiple transfected and untransfected cells, Kv2.1 and ΔC187 are correctly localized (Fig. 4, *a–f*, *Kv2.1* and *ΔC187*). Cell–cell contact itself, however, does seem to be a requirement for both localization of Kv2.1 and ΔC187 to the lateral membrane and clustering. Replating transfected cells to a low density such that individual cells are devoid of cell–cell contact reveals that Kv2.1 and ΔC187 are localized homogeneously on the cell surface (data not shown). If this sparse culture is permitted to grow in culture such that cell–cell contacts develop, the channel proteins become localized to the lateral membrane as cells divide and begin to make contacts with neighboring and daughter cells. It should also be noted that even in sparsely plated cultures, aggregated cells found in presumably de novo contact will localize Kv2.1 and ΔC187 to the lateral membrane, indicating that homogenous cell surface distribution in individual transfected cells is not a temporal artifact. ΔC318, however, never exhibits a polarized or clustered distribution, even after culturing confluent monolayers for extended periods (Scannevin, R.H., and J.S. Trimmer, unpublished observations). A similar requirement of cell–cell contact for lateral localization has been described for other basolateral proteins such as the Na^+,K^+-ATPase (Balcorova-Ständer et al., 1984; Nelson and Veshnock, 1986; Vega-Salas et al., 1987), and suggests that Kv2.1 may be participating in some type of related submembraneous cytoskeletal complex. Interestingly, the high-density clustering of Kv2.1 at regions of cell–cell contact in PC12 cells is also dependent on cell aggregation (Sharma et al., 1993).

Further evidence of interaction with one or more aspects of the MDCK cellular cytoskeleton is provided by detergent insolubility of wild-type Kv2.1 in these cells. This is in contrast to expression in COS-1 cells, where the channel protein is relatively soluble. These data correlate well with the localization model that in MDCK cells, but not in COS-1 cells, Kv2.1 is participating in a complex that not only localizes the channel to the region of cell–cell contact but also appears to render it resistant to detergent extraction. Of further interest is the result that Kv2.1 becomes more soluble when transfected cells are grown in media that contains low Ca^{2+}. Enhanced solubility and nonpolarized localization of membrane proteins in MDCK cells grown in low Ca^{2+} media is thought to reflect loss of interaction with components of the submembraneous cytoskeleton necessary for correct targeting and/or retention (Nelson and Hammerton, 1989; Nelson et al., 1990).

Consistent with the notion of an underlying cytoskeletal interaction is the intriguing interdigitated localization of Kv2.1 and actin in MDCK cells. Recent studies have demonstrated that mammalian K^+ channels of the Kv1 or *Shaker*-related subfamily can directly interact with the actin-associated PSD-95/SAP90 family of guanylate kinases (Kim et al., 1995). This interaction alone is sufficient to cocluster Kv1 K^+ channels when coexpressed with PSD-95 in COS-7 cells. While this type of interaction seems a likely candidate for promotion of clustering and detergent insolubility of Kv1 family members, Kv2.1 (a member of the Kv2 or *Shab*-related subfamily) does not contain the con-

sensus PSD-95 interaction domain identified in these studies and does not interact with PSD-95 when coexpressed in COS-1 cells (J.S. Trimmer, unpublished data). Future identification of cellular proteins important in the polarized localization and clustering of Kv2.1 will allow for important insights into the mechanisms that regulate the discrete distribution of ion channel proteins necessary for correct physiological function in excitable cells.

We thank Dr. Rolf H. Joho (University of Texas Southwestern Medical School) for the Kv2.1 cDNA. We are grateful to Dr. Deborah Brown for both the critical reading of this manuscript and invaluable assistance during the initiation and throughout the duration of this project, to Dr. William Theurkauf (SUNY Stony Brook) for expert assistance with confocal imaging, and to Dr. Michael Caplan (Yale School of Medicine, New Haven, CT) for helpful discussions.

Supported by grants from the National Institutes of Health (NS34375 and NS34383) to J.S. Trimmer. This work was also supported by Wyeth-Ayerst Research and by the Center for Biotechnology at Stony Brook, funded by the New York State Science and Technology Foundation. This work was done during the tenure of an Established Investigatorship from the American Heart Association (to J.S. Trimmer).

Received for publication 25 June 1996 and in revised form 23 August 1996.

References

Almers, W., P.R. Stanfield, and W. Stühmer. 1983. Lateral distribution of sodium and potassium channels in frog skeletal muscle: measurements with a patch clamp technique. *J. Physiol. (Lond.).* 336:261–284.

Ausubel, F.M., R. Brent, R.E. Kingston, D.D. Moore, J.G. Seidman, J.A. Smith, and K. Struhl. 1990. Transfection of DNA into eukaryotic cells: calcium phosphate transfection. *In* Current Protocols in Molecular Biology. Wiley-Interscience, New York. 9.1.1–9.1.7.

Balcorova-Ständer, J.S., S.E. Pfeiffer, S.D. Fuller, and K. Simons. 1984. Development of cell surface polarity in the epithelial Madin-Darby canine kidney (MDCK) cell line. *EMBO (Eur. Mol. Biol. Organ.). J.* 3:2687–2694.

Brewer, C.B., and M.G. Roth. 1991. A single amino acid change in the cytoplasmic domain alters the polarized delivery of influenza virus hemagglutinin. *J. Cell Biol.* 114:413–421.

Chandy, K.G., and G.A. Gutman. 1993. Nomenclature for mammalian potassium channel genes. *Trends Pharmacol. Sci.* 14:434.

Chandy, K.G., and G.A. Gutman. 1995. Voltage-gated potassium channel genes. *In* Handbook of Receptors and Ion Channels: Ligand and Voltage Gated Ion Channels. R.L. North, editor. CRC Press, Boca Raton, FL. 1–58.

Compton, T., I.E. Ivanov, T. Gottlieb, M. Rindler, M. Adesnik, and D.D. Sabatini. 1989. A sorting signal for the basolateral delivery of the vesicular stomatitis virus (VSV) G protein lies in its luminal domain: analysis of the targeting of VSV-G/influenza hemagglutinin chimeras. *Proc. Natl. Acad. Sci. USA.* 86:4112–4116.

Dotti, C.G., and K. Simons. 1990. Polarized sorting of viral glycoproteins to the axons and dendrites of hippocampal neurons in culture. *Cell.* 62:63–72.

Dotti, C.G., R.G. Parton, and K. Simons. 1991. Polarized sorting of glypiated proteins in hippocampal neurons. *Nature (Lond.).* 349:158–161.

Doyle, C., J. Sambrook, and M. Gething. 1986. Analysis of progressive deletions of the transmembrane and cytoplasmic domains of influenza hemagglutinin. *J. Cell Biol.* 103:1193–1204.

Frech, G.C., A.M. VanDongen, G. Schuster, A.M. Brown, and R.H. Joho. 1989. A novel potassium channel with delayed rectifier properties isolated from rat brain by expression cloning. *Nature (Lond.).* 340:642–645.

Froehner, S.C. 1993. Regulation of ion channel distribution at synapses. *Annu. Rev. Neurosci.* 16:347–368.

Gottardi, C.J., and M.J. Caplan. 1993. Delivery of Na^+,K^+-ATPase in polarized epithelial cells. *Science (Wash. DC).* 260:552–554.

Gottardi, C.J., L.A. Dunbar, and M.J. Caplan. 1995. Biotinylation and assessment of membrane polarity: caveats and methodological concerns. *Am. J. Physiol.* 268:F285–295.

Hamill, O.P., A. Marty, E. Neher, B. Sakmann, and F.J. Sigworth. 1981. Improved patch-clamp techniques for high-resolution current recording from cells and cell-free membrane patches. *Pflüg. Arch. Eur. J. Physiol.* 391:85–100.

Heinemann, S.H. 1983. Single Channel Recording. B. Sakmann and E. Neher, editors. Plenum Press, New York. 53–91.

Hwang, P.M., M. Fotuki, D. Bredt, A.M. Cunningham, and S.H. Snyder. 1993. Contrasting immunohistochemical localization in rat brain of two novel K^+ channels of the Shab subfamily. *J. Neurosci.* 13:1569–1576.

Johnson, D.A.G., J.R. Sportsman, and J.H. Elder. 1984. Improved technique utilizing nonfat dry milk for analysis of proteins and nucleic acids transferred to nitrocellulose. *Gene Anal. Tech.* 1:3–8.

Jurman, M.E., L.M. Boland, Y. Liu, and G. Yellen. 1994. Visual identification of individual transfected cells for electrophysiology using antibody coated beads. *BioTechniques.* 17:159–165.

Kim, E., M. Niethhammer, A. Rothschschild, Y.N. Jan, and M. Sheng. 1995. Clustering of Shaker-type K^+ channels by interaction with a family of membrane-associated guanylate kinases. *Nature (Lond.).* 378:85–88.

Li, S., V. Polonis, H. Isobe, H. Zaghouani, R. Guinea, T. Moran, C. Bona, and P. Palese. 1993. Chimeric influenza virus induces neutralizing antibodies and cytotoxic T cells against human immunodeficiency virus type 1. *J. Virol.* 67: 6659–6666.

Maizel, J.V. 1971. Polyacrylamide gel electrophoresis of viral proteins. *Methods Virol.* 5:179–246.

Maletic-Savatic, M., N.J. Lenn, and J.S. Trimmer. 1995. Differential spatiotemporal expression of K^+ channel polypeptides in rat hippocampal neurons developing in situ and in vitro. *J. Neurosci.* 15:3840–3851.

Morrow, J.S, C.D. Cianci, T. Ardito, A.S. Mann, and M. Kashgarian. 1989. Ankyrin links fodrin to the alpha subunit of Na, K-ATPase in Madin-Darby Canine Kidney Cells and in intact renal tubule cells. *J. Cell Biol.* 108:455–465.

Neame, S.J., and C.M. Isacke. 1993. The cytoplasmic tail of CD44 is required for basolateral localization in epithelial MDCK cells but does not mediate association with detergent-insoluble cytoskeleton of fibroblasts. *J. Cell Biol.* 121:1299–1310.

Nelson, W.J., and R.W. Hammerton. 1989. A membrane–cytoskeletal complex containing Na^+,K^+-ATPase, ankyrin, and fodrin in Madin-Darby canine kidney (MDCK) cells: implications for the biogenesis of epithelial cell polarity. *J. Cell Biol.* 108:893–902.

Nelson, W.J., and P.J. Veshnock. 1986. Dynamics of membrane-skeleton (fodrin) organization during development of polarity in Madin-Darby canine kidney cells. *J. Cell Biol.* 103:1751–1766.

Nelson, W.J., and P.J. Veshnock. 1987. Modulation of fodrin (membrane skeleton) stability by cell–cell contact in Madin-Darby canine kidney epithelial cells. *J. Cell Biol.* 104:1527–1537.

Nelson, W.J., E.M. Shore, A.Z. Wang, and R.W. Hammerton. 1990. Identification of a membrane–cytoskeletal complex containing the cell adhesion molecule uvomorulin (E-cadherin), ankyrin, and fodrin in Madin-Darby canine kidney epithelial cells. *J. Cell Biol.* 110:349–357.

Niethammer, M., E. Kim, and M. Sheng. 1996. Interaction between the C terminus of NMDA receptor subunits and multiple members of the PSD-95 family of membrane-associated guanylate kinases. *J. Neurosci.* 16:2157–2163.

Perney, T.M., and L.K. Kaczmarek. 1993. Expression and regulation of mammalian K^+ channel genes. *Semin. Neurosci.* 5:135–145.

Pietrini, G., Y.J. Suh, L. Edelmann, G. Rudnick, and M.J. Caplan. 1994. The axonal γ-aminobutyric acid transporter GAT-1 is sorted to the apical membranes of polarized epithelial cells. *J. Biol. Chem.* 269:4668–4674.

Rhodes, K.J., S.A. Keilbaugh, N.X. Barrezueta, K.L. Lopez, and J.S. Trimmer. 1995. Association and colocalization of K^+ channel alpha- and beta-subunit polypeptides in rat brain. *J. Neurosci.* 15:5360–5371.

Rodriguez-Boulan, E., and M. Pendergast. 1980. Polarized distribution of viral envelope glycoproteins in the plasma membrane of infected epithelial cells. *Cell.* 20:45–54.

Rodriguez-Boulan, E., and S.K. Powell. 1992. Polarity of epithelial and neuronal cells. *Annu. Rev. Cell Biol.* 8:395–427.

Sharma, N., G. D'Arcangelo, A. Kleinklaus, S. Halegoua, and J.S. Trimmer. 1993. Nerve growth factor regulates the abundance and distribution of K^+ channels in PC12 cells. *J. Cell Biol.* 123:1835–1843.

Sheng, M., M.L. Tsaur, Y.N. Jan, and L.Y. Jan. 1992. Subcellular segregation of two A-type K^+ channel proteins in rat central neurons. *Neuron.* 9:271–284.

Sheng, M., Y.J. Liao, Y.N. Jan, and L.Y. Jan. 1993. Presynaptic A-current based on heteromultimeric K^+ channels detected in vivo. *Nature (Lond.).* 365:72–75.

Sheng, M., M.L. Tsaur, Y.N. Jan, and L.Y. Jan. 1994. Contrasting subcellular localization of the Kv1.2 K^+ channel subunit in different neurons of rat brain. *J. Neurosci.* 14:2408–2417.

Shi, G., A.K. Kleinklaus, N.V. Marrion, and J.S. Trimmer. 1994. Properties of Kv2.1 K^+ channels expressed in transfected mammalian cells. *J. Biol. Chem.* 269:23204–23211.

Trimmer, J.S. 1991. Immunological identification and characterization of a delayed rectifier K^+ channel in rat brain. *Proc. Natl. Acad. Sci. USA.* 88:10764–10768.

VanDongen, A.M.J., G.C. Frech, J.A. Drewe, R.H. Joho, and A.M. Brown. 1990. Alteration and restoration of K^+ channel function by deletion at the N- and C- termini. *Neuron.* 5:433–443.

Vega-Salas, D.E., P.J.I. Salas, D. Gundersen, and E. Rodriguez-Boulan. 1987. Formation of the apical pole of epithelia Madin-Darby canine kidney cells: polarity of an apical protein is independent of tight junctions while segregation of a basolateral marker requires cell–cell interactions. *J. Cell Biol.* 104:905–916.

Wang, H., D.D. Kunkel, T.M. Martin, P.A. Schwartzkroin, and B.L. Tempel. 1993. Heteromultimeric K^+ channels in terminal and juxtaparanodal regions of neurons. *Nature.* 365:75–79.

Weiss, R.E., W.M. Roberts, W. Stuhmer, and W. Almers. 1986. Mobility of voltage-dependent ion channels and lectin receptors in the sarcolemma of frog skeletal muscle. *J. Gen. Physiol.* 87:955–983.

Zurcher, T., L. Guangxiang, and P. Palese. 1994. Mutations at palmitylation sites of the influenza virus hemagglutinin affect virus formation. *J. Virol.* 68:5748–5754.

Zurzolo, C., and E. Rodriguez-Boulan. 1993. Delivery of Na^+,K^+-ATPase in polarized epithelial cells. *Science (Wash. DC).* 260:550–552.